1998 International Computer Symposium
Workshop on Image Processing and Character Recognition
December 17-19, 1998, N.C.K.U., Tainan, Taiwan, R.O.C.

SEGMENTING THE VASCULARIZATION OF THE CANCEROUS LIVER TISSUE IMAGE

Jen-Sung Peng*, Kuo-Sheng Cheng*, and Nan-Haw Chow**

*Institute of Biomedical Engineering, ** Department of Pathology,
National Cheng Kung University, Tainan, Taiwan, ROC.
E-mail: kscheng@mail.bme.ncku.edu.tw

ABSTRACT

In this paper, it is to segment the vascularization of the liver tissue image for automated hepatocarcinoma differentiation. From the pathological significance, the area of vascularization is one of the important parameter for pathological analysis. The methods employed for vascularization segmentation are Otsu's method, Otsu_2D method, fuzzy c-means, principal component transformation/median_cut, and evolutionary autonomous agents. In the automatic diagnosis, three parameters, i.e. fractal dimension, nuclear counts, and vascularization area, are used the input feature vector for the neural networks. Two types of neural network used in the diagnosis stage are learning vector quantization and probabilistic neural network. From the results, it is shown that PCT/Median_ Cut combined with LVQ would obtain the best results for accuracy about 90%. Finally, a visual programming workspace is also developed for easy to use.

1. INTRODUCTION

Biopsy analysis is one of the most important method in clinics for hepatoma diagnosis. In the past, many histological and morphometrical indicators were investigated for analyzing the hepatocellular carcinoma images[2]. Those proposed parameters were demonstrated to be very useful and helpful in the differentiation of the normal and carcinoma liver tissue images.

In this paper, our attention are paid to quantitatively analyze the angiogenesis in liver tissue image for automated biopsy analysis There are two stages in this processing: vascularization segmentation and diagnosis stages. Several color transformations and image segmentation methods such as PCT/Median_Cut[4], Fuzzy c-means[11], Learning vector quantification neural network[16] are investigated in this study for vascularization segmentation. Then, in the diagnosis stage the neural network based approach is developed.

2. METHODS

There are two stages in this studies. One is to extract the vascularization, and the other is to diagnose. The methods used in segmentation stage are shown in Fig. 1.

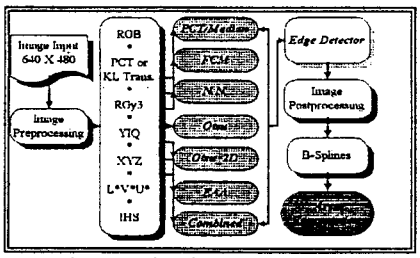

Fig. 1 The methods and procedures for vascularization segmentation.

2.1 Image Preprocessing

In the liver tissue image, color of vascularization is not uniform and noises is also contained. Thus, a median filter with 3×3 mask is used to remove the noise in the color space. From the results, it is shown that most of the noises may be significantly reduced.

2.2 Color Model Transformation

Several color models such as PCT[4], RGy3, YIQ, XYZ, and L*V*U*[7][8][9] are investigated in this paper. R and G from RGB

model and the major axis of PCT are combined as the RGy3 model. Among these model transformations, the color of vascularization is quite different each other.

2.3 Vascularization Segmentation

Several image segmention methods are employed for extracting the vascularization, including *Otsu*[13], *Otsu_2D*[5], *PCT/Median_Cut*[4], *Fuzzy C-Means (FCM)*[11], *Neural network(LVQ and PNN)*[16], and *Evolutionary Autonomous Agents(EAA)*[16]. The performances for these method are also visually compared.

2.4. Image Postprocessing

2.4.1. Curve smoothing

Edges of objects extracted from an image using the image segmentation methods are often not smooth. In this study, the vascularization should have the smooth boundary intuitively. The detected edges may be not smooth and sometimes could be broken. Therefore, two kinds of curve fitting methods, i.e. Bezier and B-Splines[10] curves, are used to generate more smooth and continuous edges. The pixels of original edges are used as the control points for these two kinds of fitting equations.

2.4.2 Line Thinning

One-pixel-wide edge is necessary in object description and image analysis. The boundary generated by B-splines is not one-pixel-wide edge. Therefore, it needs to apply the line thinning algorithm in the image postprocessing.

Many methods can be used for thinning lines, but do not guarantee that the result is a one-pixel wide and continuous line. Here, the PTA2T[12] which guarantees to produce one-pixel wide edges and preserves the connectivity of lines is applied in this paper.

2.5 Visual Programming

In the image processing field, one image is usually processed by many procedures before showing the satisfactory results. It is helpful if one can arrange the procedures as coding a program such as designing a executive flow, and using loop operators and sentential operators. In addition, the sequential procedures can be examined before execution.

In this study, many image processing procedures have been constructed as functions for users to choose. Furthermore, a workspace called Visual Programming Workspace (VPW) is created, in which the user can link different procedures together to process an image. As mentioned above, it is better to make this workspace to be a visual programming one. Therefore, a function library is built for including the image processing procedures represented as an icon. User only has to drag the icon(a procedure) out of the function library, and then the procedure will be added into the VPW. On the contrary, a procedure is removed just by dragging the icon out of the VPW. After the procedures are set up in the VPW, user nedds to build the executive file. If any illegal linkage happens, error message will be appeared in the message window as Fig. 4 and 5. The illegal linkage happens, for example, PCT/Median_Cut is only applied in color images. If it is applied to a binary one, then the error message "*PCT/Median_Cut can not be applied in gray image*" is shown. The interfaces of Function library and VPW are shown in Fig. 2 and 3.

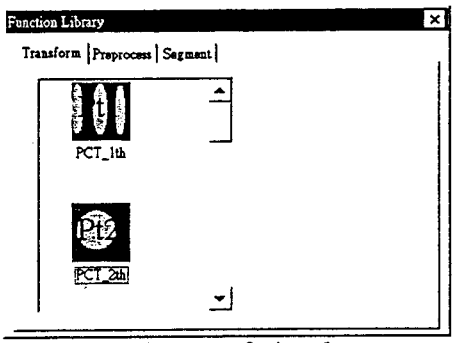

Fig. 2 Function library of visual programming.

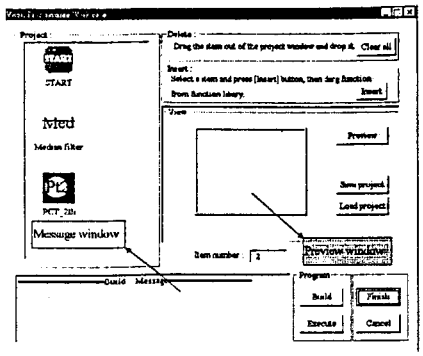

Fig. 3 Visual programming workspace.

Fig. 4 After pressing button "*Build*" VPW will check if the linkage is legal. This is a legal one.

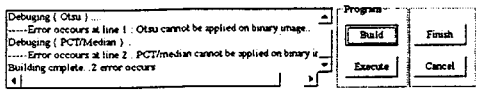

Fig. 5 This is an illegal linkage. The reason of occurring error is displayed in the message window.

2.6 Diagnosis Stage

The methods mentioned above can extract the vascularization of an image and then counts the area. The area is one of the parameters for diagnosis. According to [13], fractal dimension[1] estimated from the liver tissue image after being processed by Contrast enhancement and Edge based histogram equalization performs well in diagnosing carcinoma. Therefore, three parameters are combined as the input feature vector for Learning Vector Quantization network. The whole diagnosis mechanism is established as shown in Fig. 6.

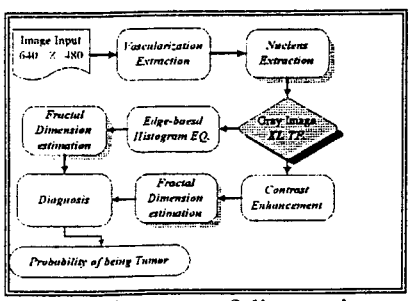

Fig. 6 Architecture of diagnosis stage.

20 subimages with the size 128 × 128 are extracted from original liver tissue image for estimating the fractal dimension. If it is tumor, a weightingg value 4.0 will be assigned; otherwise 0.0 will be assigned. Then these 20 values will be summed up and input to the sigmoid type activation function to produce the probability of being hepatocellular carcinoma. The sigmoid function is defined in the following:

$$\frac{1}{1+\exp(-2*(sum-middle))}*100$$

where sum = *summation of the* 20 *values*
$middle = 20*weight/2$

3. RESULTS AND DISCUSSION

A tissue image with hepatocarcinoma containing lots of vascularization is shown in Fig.7(a). Fig. 7(b) shows the results of applying the Otsu method with YIQ color model. Vascularization in YIQ color model are green, and Otsu is a method only for gray images. Therefore, Otsu was applied to extract vascularization on axis I which is one component of YIQ color space. The results are not bad in this case. But we can see in other cases later, the results of extracting vascularization by Otsu's method are very bad, especially in cases containing less vascularization. Fig. 7(c) is the result of PCT/Median_Cut with RGB color model. It is seen that both the cells and vascularization are extracted at the same time. Fig. 7(d) is the result of LVQ. In comparison Fig. 7(c) with Fig. 7(d), the edges of vascularization in (c) are fitted better than those in (d). Besides, the cells are not extracted in (d). Therefore, these two methods are further combined in order to eliminate cells in (c). The result is shown in Fig. 7(e). In (e), the cells are eliminated and edges of vascularization are more precise than (d). At last, the result of FCM with RGB color model was shown in Fig. 7(f). The vector (2, 2) denotes the fuzziness and number of objects, respectively. These values are empirically chosen. Both the cells and vascularization are extracted this case. For a cancerous image with omly a little vascularization. Therefore, unsupervised methods can not well perform with no existence of vascularization. Objects

other than vascularization are still extracted according to the algorithm. Such problem can still exist when we applied these kind of methods to the normal images.

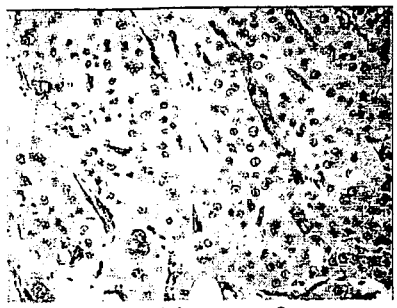

Fig. 7 (a) Original image of a tumor tissue image.

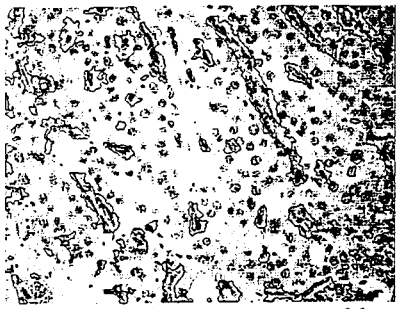

Fig. 7(b) resulting image processed by Otsu(I of YIQ)

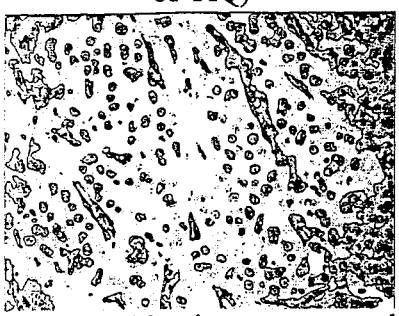

Fig. 7(c) resulting image processed by PCT/Median_Cut (RGB)

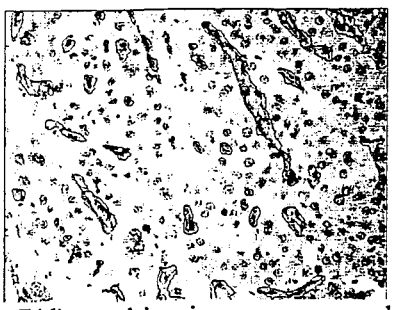

Fig. 7(d) resulting image processed by LVQ(RGy3)

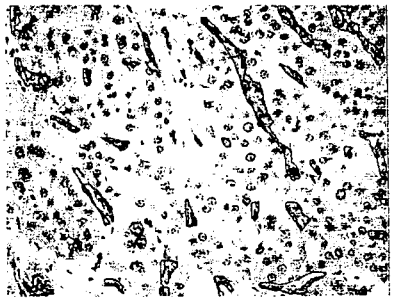

Fig.7(e) resulting image processed by PCT/Median_Cut + LVQ

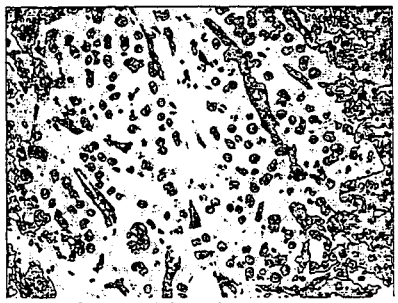

Fig. 7(f) resulting image processed by FCM(RGB) with (2 , 2)

The procedures for the accuracy assessment is summarized as follows.

Step 1 : The edge of vascularization are manually selected to be the control points of *Bezier* curve. Then, the curves is fitted.

Step 2 : The occupied area of edges is estimated.

Step 3 : The accuracy is calculated as

$$Accuracy = 1 - \frac{|A_1 - A_2|}{A_2}$$

where A_1 *is the area of the object segmented automatically.*

A_2 *is the area of the object segmented manually.*

The results show that images with more vascularization will have higher accuracy as being applied by the unsupervised segmentation methods like Otsu's method, PCT/Median_Cut, and FCM. Accuracy for LVQ and PCT/Median_Cut mehtod is not different significantly between the normal and tumor images, while unsupervised methods do. Unsupervised methods are almost useless in the normal images.

The biopsy images for the liver tissue in this study are varied case by case, and the amount of vascularization of normal images are much less than the tumor ones. Most image

segmentation approaches are based on finding the difference between objects of an image. For example, PCT/Median_Cut segments objects by different values in the principal axis. Therefore, if there are a little vascularization in an image, PCT/Median_Cut will still extract undesired objects. Another example is FCM. It separates objects by color difference in three axes and the number of objects *N*. FCM separates the three dimensional space into *N* subspace with each subspace representing one object. The problem is like PCT/Median_Cut. There is no specified subspace just for vascularization. Other methods like Otsu, Otsu_2D also have the same problem in this study. Therefore, if we want to segment the vascularization automatically, some features of vascularization are necessary. The results show that the accuracy of LVQ is much better than the other unsupervised methods.

Although PCT/Median_Cut can segment most cells and vascularization, the edges of vascularization seems more close to real ones. Therefore, LVQ and PCT/Median_Cut are combined and produce the results indeed better than those just using LVQ. It is noted that PCT/Median_Cut is applied in *RGB* color model, and the LVQ is in *RGy3* color model. The reason is that *RGy3* gives the colors between vascularization and the others much different. This color model is modified from the *PCT*. The third axis of *PCT* preserves most vascularization information good for segmentation.

As to the PCT/Median_Cut and FCM, it is a problem for choosing color number and cluster number, respectively. 3 colors are selected for PCT/Median_Cut, and 2 clusters for FCM with *RGB* color space. These values are good in the vascularization segmentation in this study. Moreover, it needs to make the objects more homogeneous using median filter. In this study, the median filter is applied to the liver tissue image several times before vascularization segmentation. The results show the extracted objects are more complete and less holes. From the results, it is shown that supervised neural network can extract vascularization more precisely than other unsupervised segmentation methods.

EAA is also used to find the edge of vascularization in this study. The initial seed points(agents) are the edge pixels extracted by some edge detection method. Therefore, they should be the edges or near the edges. S

Two kinds of neural networks are used in the this study. The training time of PNN is less than that of LVQ, but its recalling time is much more than that of LVQ. Since each training pattern will generate a node that in the hidden layer of PNN, the color of each pixel is a training pattern. Therefore, the number of nodes in the hidden layer are very large. Due to the huge hidden layer, the recalling procedure takes lots of time. An image with size 640 $\times$ 480 takes about 2.5 hours to finish the segmentation. If the number of hidden layer nodes is increased, then the results becomes very bad. On the contrary, the recalling procedures of LVQ only takes about 2 minutes with six hidden layer nodes. The color of each pixel regarded as the training pattern of PNN is not appropriate in segmentation directly. New features should be extracted as the inputs of PNN.

The results of LVQ are satisfied but there are still some modifications can be made. The initialization of weighting function between input and hidden layer is also an important subject. Here, the weighting function is initialized based on the experimental results. This is not a good way in setting the initialization. Some modified methods have been proposed in [16]. Table 1 lists the classification results with the certainty of diagnosis stage.

Table 1 The classification results with the hepatocarcinoma certainty of diagnosis stage.

Results of Diagnosis					
Case No.	**Classification**	**Certainty**	**Case No.**	**Classification**	**Cartainty**
Tc946774	Tumor	100.00	Na902355	Normal	1.87
Ta893366	Tumor	96.42	Na914901	Normal	1.87
Ta91480	Tumor	100.00	Na921062	Normal	4.24
Ta911344	Tumor	88.92	Na923220	Normal	1.87
Ta915283	Tumor	94.68	Na925033	Normal	12.68
Ta916495	Tumor	94.68	Na925876	Normal	4.24
Ta91712	Tumor	88.92	Na931043	Normal	12.68
Ta92309	Tumor	96.42	Na935501	Normal	1.87
Ta902355	Tumor	100.00	Na93945	Normal	1.87
Ta914901	Tumor	88.92	Na946774	Normal	12.68

4. CONCLUSION

In this study, different color models and image segmentation approaches are investigated in segmenting the vascularization of liver tissue image. Besides, the neural networks are also employed for the automated hepatocarcinoma diagnosis. Among all the image processing methods, PCT/Median_Cut with *RGB* color model coombined LVQ with *RGy3* color model provides the best results. The accuracy for it is about 91%. Unsupervised segmentation methods can only perform well in the cases with lots of vascularization. While its accuracy is less than 10% in the cases with little vascularization. At the diagnosis stage, four parameters are taken as the input feature vector to the probabilistic neural network. The accuracy is more than 90% in the hepatocarcinoma diagnosis. At last, a visual programming workspace is also designed and implemented for user to easily plan his image processing methods.

In practice, normal and cancerous tissues may usually be seen in the image. To distinguish the normal from cancerous region is also an interesting subject. Based on our previous results of fractal analysis of the hepatocarcinoma, the fractal dimension may be a good parameter for dividing the liver tissue image into normal and cancerous parts. Moreover, merge and split algorithm is also a good way to solve this problem.

The helpful information for pathologist in biopsy analysis is the morphological parameters of cells, neuclei, and area of vascularization. Therefore, a knowledge base system containing these information will be very useful in clinical diagnosis as well as pathologist training. It may be accomplished using the artificial intelligence approach.

ACKNOWLEDGMENT

This work is partly supported by the National Science Council, ROC under the Grant#NSC87-2213-E006-066, NSC86-2213-E006-027, and NSC85-2213-E006-076. This is part of master thesis of Jen-Sung Peng which is awarded by 1998 Dragon Master Thesis Award, Acer Foundation.

REFERENCES

[1] N. Sarkar and B. B. Chaudhuri, "An efficient differential box-counting approach to compute fractal dimensions of image," IEEE Trans. Syst. Man. & Cybern., vol. 24, no. 1, pp. 115-120, 1994.

[2] Y. Nagato, F. Kondo, Y. Kondo, M. Ebara, and M. Ohta, "Histological and morphometrical indicators for a biopsy diagnosis of well-differentiated

hepatocellular carcinoma," Hepatology, vol. 14, no. 3, pp. 472-478, 1991.

[3] S. E. Umbaugh, R. H. Moss, W. V. Stoecker, and G. A. Hance, "Automatic color segmentation algorithms with Application to Skin Tumor Feature Identification," IEEE Eng. Med. Biol., vol. 12, no. 3, pp. 75-82, 1993.

[4] G. A. Hance, S. E. Umbaugh, R. H. Moss, and W. V. Stoecker, "Unsupervised color image segmentation: with application to skin tumor borders ," IEEE Eng. Med. Biol., vol. 15, no. 1, pp. 104-111, 1996.

[5] J. Liu, W. Li, and Y. Tian, "Automatic thresholding of gray-level pictures using two-dimension Otsu method," Proc. Int. Conf. Circuits & Systems, vol. 1, pp. 325-327, 1991.

[6] J. Liu, Y. Y. Tang, and Y. C. Cao, "An evolutionary autonomous agents approach to image feature extraction," IEEE Trans. Evolut. Comput., vol. 1, no. 2, pp. 141-158, 1997.

[7] D. C. Tseng and C. H. Chang, "Color segmentation using perceptual attributes," Proc. 11th IEEE IAPR Int. Conf. Image, Speech and Signal Analysis, vol. 3, pp. 228-231, 1992.

[8] T. Carron and P. Lambert, "Symbolic fusion of hue-chroma-intensity features for region segmentation," Proc. 3rd IEEE Int. Conf. Image Processing, vol. 1, pp. 971-974, 1996.

[9] J. H. Lee, B. H. Chang, and S. D. Kim, "Comparison of colour transformations for image segmentation," Electronics Letters, vol. 30, no. 20, pp. 1660-1661, 1994.

[10] Z. Huang and F. S. Cohen, "Affine-invariant B-spline moments for curve matching," IEEE Trans. Image Proc., vol. 5, no. 10, pp. 1473-1480, 1996.

[11] X. L. Xie and G.Beni, "A validity measure for fuzzy clustering," IEEE Trans. Patt. Anal. Mach. Intell., vol. 13, no. 8, pp. 841-847, 1991.

[12] Y. Y. Zhang and P. S. P. Wang, "A parallel thinning algorithm with two-subiteration that generates one-pixel-wide skeletons," Proc. IEEE 13th Int. Conf. Pattern Recognition, vol. 3, pp. 457-461, 1996.

[13] R. Sun, *The Quantification Analysis of Liver Tissue Image*, Master Thesis, National Cheng Kung University, Tainan, TAIWAN, ROC, 1996.

[14] S.-S. Huang, *Automatic Hepatocellular Image Analysis for Morphological Parameters*, Master Thesis, National Cheng Kung University, Tainan, TAIWAN, ROC, 1997.

[15] R. C. Gonzalez and R. E. Woods, *Digital Image Processing*, Addison-Wesley, 1992.

[16] S. Haykin, *Neural Networks: A Comprehensive Foundation*, Macmillan, 1994.